Evolution of degree of polarization of partially coherent beams propagation in slant and horizontal atmospheric turbulence

X. Z. Ke, J. Wang & M. J. Wang

Indian Journal of Physics

ISSN 0973-1458
Volume 93
Number 6

Indian J Phys (2019) 93:691-699
DOI 10.1007/s12648-018-1336-8

Springer

Indian J Phys (June 2019) 93(6):691–699
https://doi.org/10.1007/s12648-018-1336-8

ORIGINAL PAPER

Evolution of degree of polarization of partially coherent beams propagation in slant and horizontal atmospheric turbulence

X Z Ke[1,2], J Wang[1]* and M J Wang[1]

[1]School of Automation and Information Engineering, Xi'an University of Technology, Xi'an 710048, China

[2]Faculty of Physics and Telecommunications Engineering, Shaanxi University of Technology, Hanzhong 723003, China

Received: 02 April 2018 / Accepted: 16 August 2018 / Published online: 23 November 2018

Abstract: In this paper, the analytical expressions for the degree of polarization (DoP) of the electromagnetic Gaussian Schell-model (GSM) beam propagating along a slant path in atmospheric turbulence are obtained. The expressions are used to analyze factors such as the waist radius, amplitude ratio, wavelength, and refractive-index structure constant of the polarization properties of the GSM beam, and we come to some new conclusions. The main results that when the components of the waist radius are equal ($\sigma_x = \sigma_y$), there is a waist radius within 2 cm $< \sigma_x <$ 4 cm that can provide the most concentrated DoP distribution, and the axis point DoP will eventually approach the initial value as the transmission distance increases, implying that it exhibits self-recovering characteristics. In addition, compared to a horizontal path, the DoP distribution of the GSM beam propagating along a slant path is more concentrated, and the propagation distance corresponding to the maximum axis point DoP is longer. Therefore, when the GSM beam propagates along a slant path, the detector can receive information at longer distances. The research results provide a theoretical support for the control of the polarization state of local beam in coherent optical communication systems.

Keywords: Coherent optical communication systems; Polarization control; Atmospheric turbulence

PACS Nos.: 42.25.Ja; 42.25.Kb; 42.25.Dd; 42.68.Bz

1. Introduction

Polarization is an important property of laser beams and has been extensively studied because of its several important applications in remote sensing, polarization control, and target detection and recognition [1–3]. When laser beams propagate in atmospheric turbulence, the refractive-index random fluctuation affects the polarization properties [4–6]. The study of the polarization properties of laser beams propagating in atmospheric turbulence is thus of great significance.

At present, the theoretical study of polarization properties is based on the cross-spectral density matrix (CSDM) [7–12]. Wolf et al. proposed a unified theory of coherence and polarization, which is of great significance for studying the polarization properties, and derived the expression for the degree of polarization (DoP) and direction of polarization of a beam propagating in atmospheric turbulence [5, 13–15]; other related studies have discovered that this change is closely related to the light source parameters and turbulence intensity [16]. Zhao et al. obtained a suitable condition for a Gaussian Schell-model (GSM) beam to maintain the state of polarization (SoP). Specifically, the GSM beam maintains the SoP while propagating when three spectral correlation widths (δ_{xx}, δ_{yy}, and δ_{xy}) are equal and the beam parameters $\sigma_x = \sigma_y$ [17]; an experimental study on the modulation of the Stokes parameters confirms this conclusion [18]. Zhao et al. investigated the evolution and modulation in the spectral DoP of a stochastic electromagnetic GSM beam in atmospheric turbulence [19–21]. Cai found that the M^2-factor of a stochastic electromagnetic GSM beam is primarily related to its initial DoP [22]. Zhang et al. focused on the polarization properties of GSM beams propagating through the anisotropic non-Kolmogorov turbulence of a marine atmosphere [23, 24].

In recent years, several researchers have studied two aspects of polarization properties. One is the change in the

*Corresponding author, E-mail: jiaolun216@163.com

polarization properties of various beams [25–28], and the other is the change in the polarization properties of a beam propagating along different paths [10–13, 25–29]. Because of the different turbulence mechanisms in the slant path and horizontal path, the polarization properties of the beam are different. Using the unified theory of coherence and polarization, this paper presents the derivation of the expressions for the DoP and compares the difference in polarization properties of a GSM beam propagating through horizontal and slant paths in atmospheric turbulence. Our study is important for controlling the polarization of laser beams in a coherent optical communication system.

2. Theory

Based on the unified theory of coherence and polarization [13], a beam is generated by a source located in the $z = 0$ plane (the source plane) and propagates close to the positive z-axis into the half-space $z > 0$, as shown in Fig. 1. The CSDM is given by [5]

$$\overleftrightarrow{W}(\boldsymbol{\rho}_1,\boldsymbol{\rho}_2;z) \equiv W_{ij}(\boldsymbol{\rho}_1,\boldsymbol{\rho}_2;z) = \begin{bmatrix} W_{xx}(\boldsymbol{\rho}_1,\boldsymbol{\rho}_2;z) & W_{xy}(\boldsymbol{\rho}_1,\boldsymbol{\rho}_2;z) \\ W_{yx}(\boldsymbol{\rho}_1,\boldsymbol{\rho}_2;z) & W_{yy}(\boldsymbol{\rho}_1,\boldsymbol{\rho}_2;z) \end{bmatrix}, \quad (1)$$

where $W_{ij}(\boldsymbol{\rho}_1,\boldsymbol{\rho}_2;z) = \left\langle E_i(\boldsymbol{\rho}_1;z)E_j^*(\boldsymbol{\rho}_2;z)\right\rangle$ and $(i,j = x,y)$. E_i and E_j are respectively the components of the random optical field in the x- and y-directions, and the asterisk represents the complex conjugate. $\boldsymbol{\rho}_1$ and $\boldsymbol{\rho}_2$ denote two points in the receiver plane at $z > 0$, and $<\cdot>$ denotes the ensemble average.

When $\boldsymbol{\rho}_1 = \boldsymbol{\rho}_2 = \boldsymbol{\rho}$, by using the generalized Stokes parameters [30], the DoP of the received beam is expressed as

$$P(\boldsymbol{\rho};z) = \frac{\sqrt{S_1^2 + S_2^2 + S_3^2}}{S_0} \quad (2)$$

where S_0, S_1, S_2, and S_3 are the Stokes parameters for the random beam and can be expressed by the elements of the CSDM:

$$\begin{aligned} S_0 &= W_{xx}(\boldsymbol{\rho},\boldsymbol{\rho};z) + W_{yy}(\boldsymbol{\rho},\boldsymbol{\rho};z)\, S_1 = W_{xx}(\boldsymbol{\rho},\boldsymbol{\rho};z) - W_{yy}(\boldsymbol{\rho},\boldsymbol{\rho};z) \\ S_2 &= W_{xy}(\boldsymbol{\rho},\boldsymbol{\rho};z) + W_{yx}(\boldsymbol{\rho},\boldsymbol{\rho};z)\, S_3 = i\left[W_{yx}(\boldsymbol{\rho},\boldsymbol{\rho};z) - W_{xy}(\boldsymbol{\rho},\boldsymbol{\rho};z)\right]. \end{aligned} \quad (3)$$

In the source plane $z = 0$, the elements of the CSDM of the GSM source can be expressed by [31, 32]

$$W_{ij}(\boldsymbol{r}_1,\boldsymbol{r}_2;0) = A_iA_jB_{ij}\exp\left[-\left(\frac{\boldsymbol{r}_1^2}{4\sigma_i^2} + \frac{\boldsymbol{r}_2^2}{4\sigma_j^2}\right)\right]\exp\left(-\frac{|\boldsymbol{r}_1 - \boldsymbol{r}_2|^2}{2\delta_{ij}^2}\right), \quad (4)$$

where $\mathbf{r}_1$ and $\mathbf{r}_2$ denote two points in the transverse source plane at $z = 0$. A_i and A_j are the amplitudes of the GSM beam in the x- and y-directions, respectively, and σ_i and σ_j are the waist radii in the x- and y-directions, respectively. δ_{ij} is the coherence length of the GSM beam, and $\delta_{ij} = \delta_{ji}$. B_{ij} satisfies the following conditions [6]:

$$B_{ij} = 1 \quad \text{when } i = j; \quad |B_{ij}| \le 1 \quad \text{when } i \ne j; \quad B_{ij} = B_{ji}^*, \quad (5)$$

According to the extended Huygens–Fresnel principle [28], when the GSM beam propagates from the source plane ($z = 0$) to the receiver plane ($z = L$), the elements of the CSDM is expressed by

$$\begin{aligned} W_{ij}(\boldsymbol{\rho}_1,\boldsymbol{\rho}_2;z) = A_iA_jB_{ij}\left(\frac{k}{2\pi L}\right)^2 \int \mathrm{d}\boldsymbol{r}_1 \int \mathrm{d}\boldsymbol{r}_2 \\ \times \exp\left[-\frac{\boldsymbol{r}_1^2}{4\sigma_i^2} + \frac{\boldsymbol{r}_2^2}{4\sigma_j^2}\right)\right]\exp\left(-\frac{|\boldsymbol{r}_1 - \boldsymbol{r}_2|^2}{2\delta_{ij}^2}\right) \\ \times \exp\left[-\frac{ik}{2L}\left(|\boldsymbol{\rho}_1 - \boldsymbol{r}_1|^2 - |\boldsymbol{\rho}_2 - \boldsymbol{r}_2|^2\right)\right] \\ \times \langle \exp[\psi(\boldsymbol{\rho}_1,\boldsymbol{r}_1) + \psi^*(\boldsymbol{\rho}_2,\boldsymbol{r}_2)]\rangle, \end{aligned} \quad (6)$$

where L is the propagation distance and k is the optical wave number related to the wavelength λ by $k = 2\pi/\lambda$. $\psi(\boldsymbol{\rho}, \boldsymbol{r})$ represents the random part of the complex phase of a spherical wave propagating in a turbulent atmosphere from the point $(\boldsymbol{r}, 0)$ to $(\boldsymbol{\rho}, L)$, and $<\exp[\psi(\boldsymbol{\rho}_1, \boldsymbol{r}_1) + \psi^*(\boldsymbol{\rho}_2, \boldsymbol{r}_2)]>$ is written as

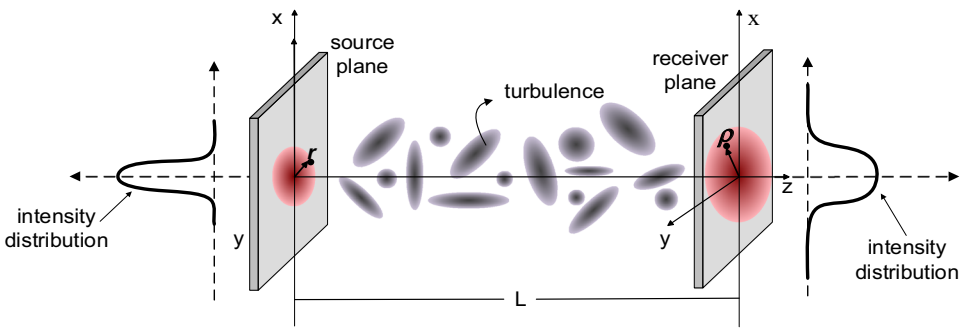

Fig. 1 Beam propagating in atmospheric turbulence

$$\langle \exp[\psi(\boldsymbol{\rho}_1,\boldsymbol{r}_1)+\psi^*(\boldsymbol{\rho}_2,\boldsymbol{r}_2)]\rangle = \exp\left[-\frac{1}{2}D_\psi(\boldsymbol{\rho}_1-\boldsymbol{\rho}_2,\boldsymbol{r}_1-\boldsymbol{r}_2)\right], \tag{7}$$

where $\underline{D}_\psi(\boldsymbol{\rho}_1-\boldsymbol{\rho}_2, \boldsymbol{r}_1-\boldsymbol{r}_2)$ represents the wave structure function [33]:

$$\begin{aligned} D_\psi(\boldsymbol{\rho}_1-\boldsymbol{\rho}_2,\boldsymbol{r}_1-\boldsymbol{r}_2) &= 8\pi^2k^2\sec\eta \\ &\times \int_0^1\int_0^\infty \kappa\phi_n(\kappa,h)\{1-J_0[|(1-\xi)(\boldsymbol{\rho}_1-\boldsymbol{\rho}_2) \\ &+\xi(\boldsymbol{r}_1-\boldsymbol{r}_2)|\kappa]\}\mathrm{d}\kappa\mathrm{d}\xi, \end{aligned} \tag{8}$$

where $J_0(x)$ is the Bessel function of the first kind and zeroth order, η is the zenith angle, κ is the scale of turbulence, and $\phi_n(\kappa, h)$ is the spectrum of the refractive-index fluctuations. However, $J_0(x)$ is approximated by the first two terms in the power series expansion [34], $J_0(x) = 1 - x^2/4$, thus, Eq. (8) can be simplified as

$$\begin{aligned} D_\psi(\boldsymbol{\rho}_1-\boldsymbol{\rho}_2,\boldsymbol{r}_1-\boldsymbol{r}_2) &= 2\pi^2k^2\sec\eta\int_0^1\int_0^\infty \kappa^3\phi_n(\kappa,h) \\ &\times\left\{\left[(1-\xi)^2(\boldsymbol{\rho}_1-\boldsymbol{\rho}_2)^2+2(1-\xi)\xi(\boldsymbol{\rho}_1-\boldsymbol{\rho}_2)(\mathbf{r}_1-\mathbf{r}_2)\right.\right. \\ &\left.\left.+\xi^2(\boldsymbol{r}_1-\boldsymbol{r}_2)^2\right]\right\}\mathrm{d}\kappa\mathrm{d}\xi, \end{aligned} \tag{9}$$

Command parameters M_1, M_2, M_3 are respectively represented as

$$\begin{cases} M_1 = 2\pi^2k^2\sec\eta\int_0^1\int_0^\infty \phi_n(\kappa,h)(1-\xi)^2\kappa^3\mathrm{d}\kappa\mathrm{d}\xi \\ M_2 = 4\pi^2k^2\sec\eta\int_0^1\int_0^\infty \phi_n(\kappa,h)(1-\xi)\xi\kappa^3\mathrm{d}\kappa\mathrm{d}\xi \\ M_3 = 2\pi^2k^2\sec\eta\int_0^1\int_0^\infty \phi_n(\kappa,h)\xi^2\kappa^3\mathrm{d}\kappa\mathrm{d}\xi \end{cases}. \tag{10}$$

then, Eq. (9) is simplified as

$$\begin{aligned} D_\psi(\boldsymbol{\rho}_1-\boldsymbol{\rho}_2,\boldsymbol{r}_1-\boldsymbol{r}_2) &= M_1(\boldsymbol{\rho}_1-\boldsymbol{\rho}_2)^2+M_2(\boldsymbol{\rho}_1-\boldsymbol{\rho}_2) \\ &\cdot(\boldsymbol{r}_1-\boldsymbol{r}_2)+M_3(\boldsymbol{r}_1-\boldsymbol{r}_2)^2, \end{aligned} \tag{11}$$

The slant path includes the uplink and downlink paths. When the beam propagates along the uplink path, $\xi = 1 - (h - h_0)/(H - h_0)$, where H is the height of the receiver and h_0 is the height of the optics source. In the condition of the downlink path, $\xi = (h - h_0)/(H - h_0)$, where H is the height of the optics source and h_0 is the height of the receiver. If the beam propagates along the horizontal path, Eq. (10) dictates that $M_3 = 2/3\pi^2k^2z\int_0^\infty \kappa^3\phi_n(\kappa, h = 0)\mathrm{d}\kappa$ and $M_1 = M_2 = 0$. In this study, we focused on the uplink path and horizontal path. We analyzed the inner- and outer-scale effects through the use of the modified von Karman spectrum model [33]:

$$\phi_n(\kappa,h) = 0.033C_n^2(h)\frac{\exp(-\kappa^2/\kappa_m^2)}{(\kappa^2+\kappa_0^2)^{11/6}}, \tag{12}$$

where $\kappa_m = 5.92/l_0$, $\kappa_0 \approx 2\pi/L_0$, and l_0 and L_0 represent the inner scale and outer scale, respectively. $C_n^2(h)$ is the refractive-index structure constant. The ITU-R model is described as [33]

$$\begin{aligned} C_n^2(h) &= 8.148\times10^{-56}v_{\mathrm{RMS}}^2h^{10}\exp\left(-\frac{h}{1000}\right)+2.7 \\ &\times10^{-16}\exp\left(-\frac{h}{1500}\right)+C_0\exp\left(-\frac{h}{100}\right). \end{aligned} \tag{13}$$

where $v_{\mathrm{RMS}} = (v_g^2 + 30.69v_g + 348.91)^{1/2}$ is the wind speed along the vertical path, v_g is the ground wind speed, and C_0 is the nominal value of the ground level (typically 1.7×10^{-14} $\mathrm{m}^{-2/3}$).

Substituting Eqs. (11) and (7) into Eq. (6) and using $\boldsymbol{\rho}_1 = \boldsymbol{\rho}_2 = \boldsymbol{\rho}$, the expressions for the CSDM of the beam in the receiver plane $z > 0$ is obtained by

$$\begin{aligned} W_{ij}(\boldsymbol{\rho},\boldsymbol{\rho};z) &= A_iA_iB_{ij}\left(\frac{k}{2\pi z}\right)^2\int\mathrm{d}\boldsymbol{r}_c\int\mathrm{d}\boldsymbol{r}_d \\ &\times\exp\left[-\left(\frac{1}{\alpha_{ij}^2}\boldsymbol{r}_c^2+\frac{1}{\beta_{ij}}\boldsymbol{r}_c\boldsymbol{r}_d+\frac{1}{4\alpha_{ij}^2}\boldsymbol{r}_d^2\right)\right] \\ &\times\exp\left(-\frac{\boldsymbol{r}_d^2}{2\delta_{ij}^2}\right)\exp\left[\frac{ik}{L}(\boldsymbol{r}_c\boldsymbol{r}_d-\rho\boldsymbol{r}_d)\right] \\ &\times\exp\left[-M_3\boldsymbol{r}_d^2\right], \end{aligned} \tag{14}$$

where $r_c = 1/2(r_1 + r_2), r_d = r_1 - r_2$, $1/\alpha_{ij}^2 1/\left(4\sigma_i^2\right) + 1/\left(4\sigma_j^2\right)$ and $1/\beta_{ij}^2 = 1/\left(4\sigma_i^2\right) - 1/\left(4\sigma_j^2\right)$. The variables $\boldsymbol{r}_c$ and $\boldsymbol{r}_d$ are sequentially integrated; namely, Eq. (14) reduces to

$$W_{ij}(\boldsymbol{\rho},\boldsymbol{\rho};z) = \frac{A_iA_iB_{ij}}{\Delta_{ij}^2}\exp\left(-\frac{\boldsymbol{\rho}^2}{\Delta_{ij}^2\cdot\alpha_{ij}^2}\right), \tag{15}$$

$$\Delta_{ij}^2 = 1-\frac{2i}{k\beta_{ij}}z+\frac{1}{k^2}\left[\left(\frac{1}{\chi_{ij}^2}+M_3\right)\frac{4}{\alpha_{ij}^2}-\frac{1}{\beta_{ij}^2}\right]z^2, \tag{16}$$

$$\frac{1}{\chi_{ij}^2} = \frac{1}{4\alpha_{ij}^2}+\frac{1}{2\delta_{ij}^2}. \tag{17}$$

From Eqs. (3) and (15), the Stokes parameters of the beam in the receiver plane $z > 0$ is expressed by

$$
\begin{aligned}
S_0 &= \frac{A_x^2}{\Delta_{xx}^2}\exp\left(-\frac{\boldsymbol{\rho}^2}{\Delta_{xx}^2\cdot\alpha_{xx}^2}\right)+\frac{A_y^2}{\Delta_{yy}^2}\exp\left(-\frac{\boldsymbol{\rho}^2}{\Delta_{yy}^2\cdot\alpha_{yy}^2}\right)\\
S_1 &= \frac{A_x^2}{\Delta_{xx}^2}\exp\left(-\frac{\boldsymbol{\rho}^2}{\Delta_{xx}^2\cdot\alpha_{xx}^2}\right)-\frac{A_y^2}{\Delta_{yy}^2}\exp\left(-\frac{\boldsymbol{\rho}^2}{\Delta_{yy}^2\cdot\alpha_{yy}^2}\right)\\
S_2 &= \frac{A_xA_yB_{xy}}{\Delta_{xy}^2}\exp\left(-\frac{\boldsymbol{\rho}^2}{\Delta_{xy}^2\cdot\alpha_{xy}^2}\right)+\frac{A_yA_xB_{yx}}{\Delta_{yx}^2}\exp\left(-\frac{\boldsymbol{\rho}^2}{\Delta_{yx}^2\cdot\alpha_{yx}^2}\right)\\
S_3 &= i\left[\frac{A_yA_xB_{yx}}{\Delta_{yx}^2}\exp\left(-\frac{\boldsymbol{\rho}^2}{\Delta_{yx}^2\cdot\alpha_{yx}^2}\right)-\frac{A_xA_yB_{xy}}{\Delta_{xy}^2}\exp\left(-\frac{\boldsymbol{\rho}^2}{\Delta_{xy}^2\cdot\alpha_{xy}^2}\right)\right].
\end{aligned}
\tag{18}
$$

From Eqs. (2) and (17), the axis point DoP in the receiver plane $z > 0$ is given by

$$
P(\boldsymbol{\rho}=0;z)=\frac{\sqrt{\left(\frac{A_x^2}{A_y^2}\frac{\Delta_{yy}^2}{\Delta_{xx}^2}-1\right)^2+4\left|B_{xy}\right|^2\frac{A_x^2}{A_y^2}\frac{\Delta_{yy}^4}{\Delta_{xy}^2\Delta_{yx}^2}}}{\frac{A_x^2}{A_y^2}\frac{\Delta_{yy}^2}{\Delta_{xx}^2}+1},
\tag{19}
$$

where $A_2\ x/A_2\ y = I_x/I_y$ is the ratio of the intensity in the source plane. As can be seen from Eq. (19), the axis point DoP of the beam in the receiver plane is related to $A_2\ x/A_2\ y$ and is not directly related to the single A_x and A_y.

3. Results and discussion

According to Eqs. (2), (18), and (19), we will analyze the influence of the waist radius, amplitude ratio, wavelength, and refractive-index structure constant on the polarization properties of the beam in the receiver plane. In the following numerical calculations, $B_{ij} = 0.5\exp(i\pi/4)$, $\lambda = 1.06$ μm, $\delta_{xx} = 0.02$ m, $\delta_{yy} = 0.01$ m, $\sigma_x = \sigma_y = 0.01$ m, $A_x/A_y = 1$, $\delta_{xy} = \delta_{yx} = 0.025$ m, $C2n = 1.7 \times 10^{-14}$ m$^{-2/3}$, $z = 10$ km, and $\sigma = \pi/3$. The coherent length is satisfied by [35]

$$
\max\left\{\delta_{xx},\delta_{yy}\right\}\le\delta_{xy}\le\min\left\{\delta_{xx}\Big/\left|B_{xy}\right|^{0.5},\delta_{yy}\Big/\left|B_{xy}\right|^{0.5}\right\}.
\tag{20}
$$

3.1. Influence of waist radius

Figure 2 presents the DoP distribution of the receiver beam when the waist radius of the source beam is different in the x- and y-directions, and Fig. 4 shows the variation in the axis point DoP of the receiver beam with propagation distance.

Figure 2(a)–(c) presents the DoP distribution of the GSM beam propagating along slant and horizontal paths when $z = 10$ km. It can be seen that the DoP distribution of the GSM beam propagating along the slant path is more concentrated than that along the horizontal path. Because of the difference in the turbulence term M_3 between the slant and horizontal paths, in Eq. (10), the turbulence term M_3 of the slant path is smaller than that of the horizontal path. In addition, the DoP of the GSM beam propagating along the slant path is close to 1 when the off-axis distance is relatively small. Comparing Fig. 2(a), (b), and (c), when $\sigma_x = \sigma_y$, the DoP distribution first concentrates and then diffuses with the increase in waist radius. There is a waist radius within 2 cm $< \sigma_x <$ 4 cm that can provide the most concentrated DoP distribution. That is, this waist radius makes the DoP of the receiver beam close to a constant value of 1 when the off-axis distance is the smallest. In order to more effectively prove this phenomenon, we calculate the off-axial distance corresponding to the DoP equal to 1, as shown in Fig. 3. Therefore, these conclusions can be more effectively obtained using Fig. 3. In addition, the DoP distribution is more concentrated when $\sigma_x < \sigma_y$, whereas it is more diffuse when $\sigma_x > \sigma_y$.

For different σ_x and σ_y, the changes in the axis point DoP of the GSM beam propagating along a slant path and horizontal path with propagation distance are shown in Fig. 4. The results indicate that the propagation distance corresponding to the maximum axis point DoP of the GSM beam propagating along a slant path is longer than that along a horizontal path. The propagation distance corresponding to the maximum axis point DoP will increase with the waist radius. Comparing Fig. 4(a), (b), and (c), it can be seen that when $\sigma_x = \sigma_y$, the axis point DoP tends toward the initial value after propagating over a long distance, implying that it exhibits self-recovery characteristics as the propagation distance increases. By contrast, when $\sigma_x \neq \sigma_y$, the axis point DoP tends toward a constant value that differs from the initial value. This is because the waist radius of the source beam is different in the x- and y-directions, and the influences of turbulence are different.

3.2. Influence of amplitude ratio

Figure 5 presents the DoP distribution of the receiver beam when the amplitude ratio is different in the x- and y-directions, and Fig. 6 shows the variation in the axis point DoP of the receiver beam with propagation distance.

Figure 5(a)–(c) presents the DoP distributions of a GSM beam propagating along a slant path and horizontal path, where A_x/A_y take different values. The DoP distribution is similar to the result in Fig. 2, where the DoP distribution of the GSM beam propagating along a slant path is more concentrated than that along a horizontal path. Comparing Fig. 5(a), (b), and (c), it can be seen that the range of change of the DoP distribution is small when $A_x/A_y < 1$, and that of the DoP distribution is relatively large when $A_x/A_y > 1$. However, the DoP distribution is more concentrated as the amplitude ratio decreases. Specifically, the smaller the amplitude ratio, the more quickly the DoP reaches 1 when the smaller the off-axis distance.

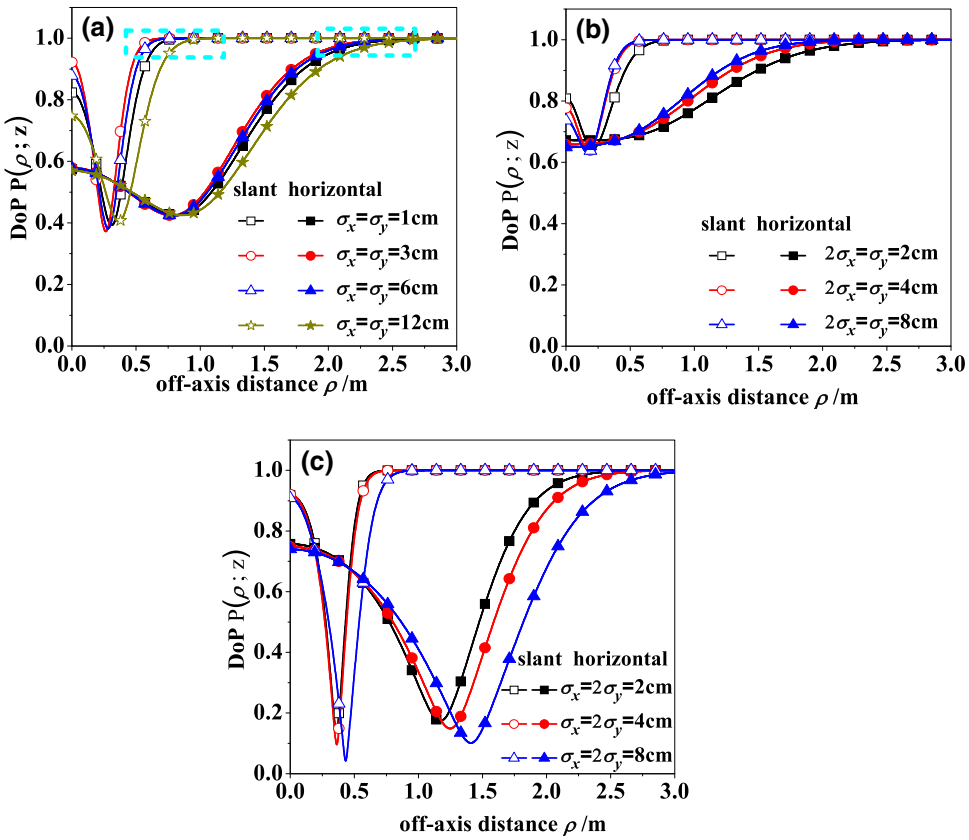

Fig. 2 DoP distributions P(ρ; z) for different waist radii σ_x and σ_y, (**a**) $\sigma_x = \sigma_y$; (**b**) $\sigma_x < \sigma_y$; (**c**) $\sigma_x > \sigma_y$

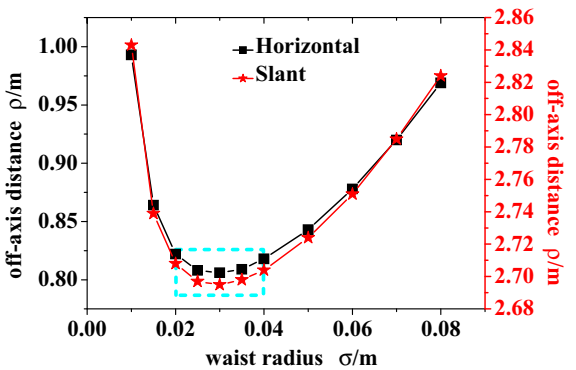

Fig. 3 Off-axial distance ρ corresponding to the DoP equal to 1 when $\sigma_x = \sigma_y$

Figure 6(a)–(c) shows the change in the DoP of a GSM beam propagating along a slant path and horizontal path with propagation distance, where A_x/A_y take different values. The conclusion is similar to the result in Fig. 4. The propagation distance corresponding to the maximum axis point DoP of the GSM beam propagating along a slant path is longer than that propagating along a horizontal path. Comparing Fig. 6(a), (b), and (c), the range of change of the axis point DoP is maximum with the increase in propagation distance when $A_x/A_y = 1$. The axis point DoP will increase in $z = 0$ with the decrease in amplitude ratio when $A_x/A_y < 1$; however, the reverse is the case when $A_x/A_y > 1$.

3.3. Influence of wavelength

Figure 7 presents the DoP distribution of the receiver beam when the wavelength is different, and Fig. 8 shows the variation in the axis point DoP of the receiver beam with propagation distance.

It can be concluded from Fig. 7 that the DoP distribution of the GSM beam propagating along a slant path is more concentrated than that along a horizontal path under the condition of the same wavelength. And, the longer the wavelength, the more concentrated the DoP distribution of the receiver beam. It can be seen from Fig. 8 that under the condition of the same wavelength, compared to a horizontal path, the detector can receive the information from a farther distance when the GSM beam propagates along a slant path. In addition, the longer the wavelength, the larger the range of change of the axis point DoP.

3.4. Influence of refractive-index structure constant

Figure 9 presents the DoP distribution of the receiver beam when the refractive-index structure constant is different,

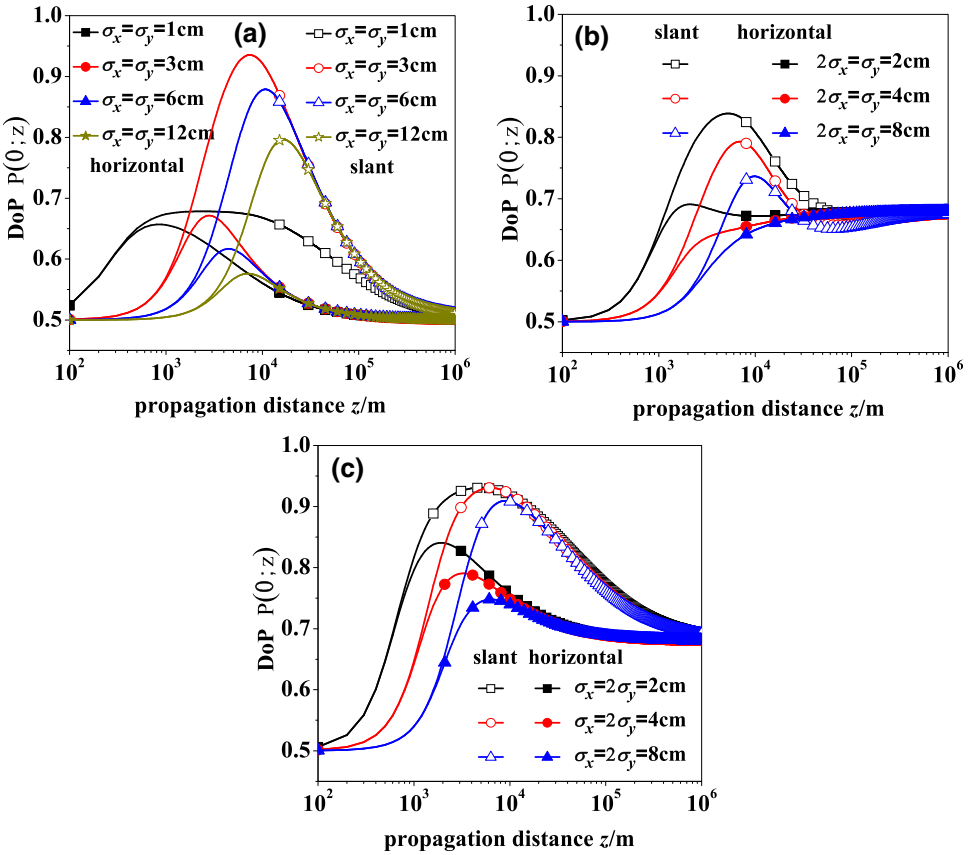

Fig. 4 Axis point DoP P(0; z) with the change in propagation distance z for different waist radii σ_x and σ_y, (**a**) $\sigma_x = \sigma_y$; (**b**) $\sigma_x < \sigma_y$; (**c**) $\sigma_x > \sigma_y$

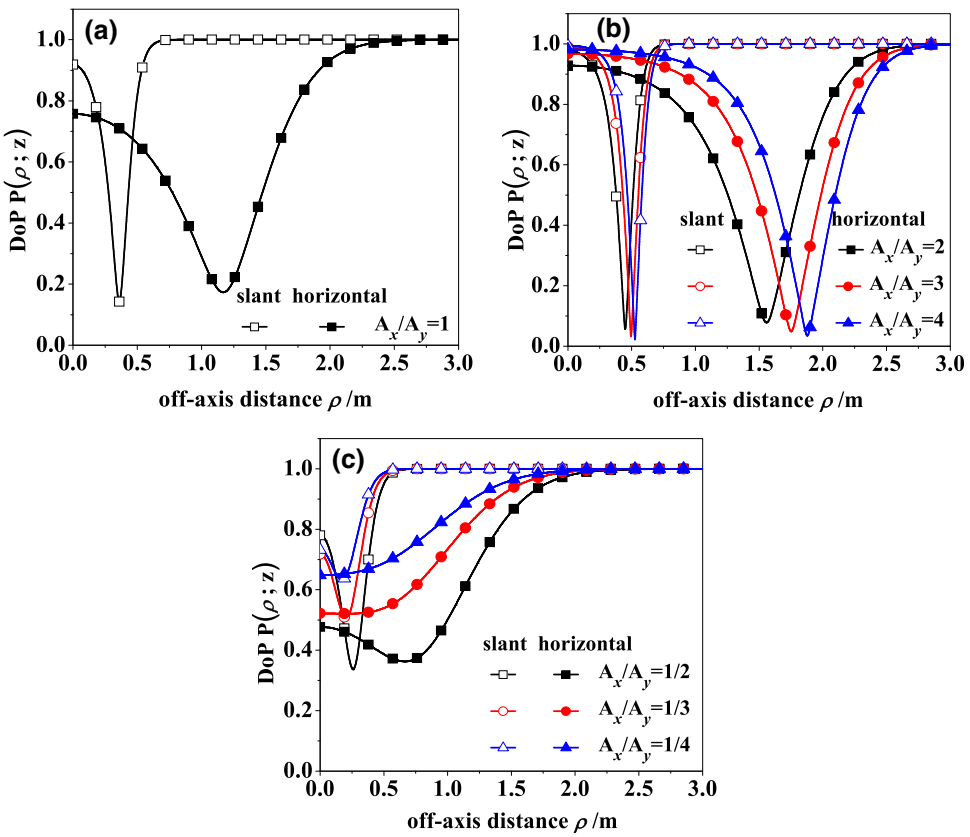

Fig. 5 DoP distributions P(ρ; z) for different amplitude ratios A_x/A_y, (**a**) $A_x/A_y = 1$; (**b**) $A_x/A_y > 1$; (**c**) $A_x/A_y < 1$

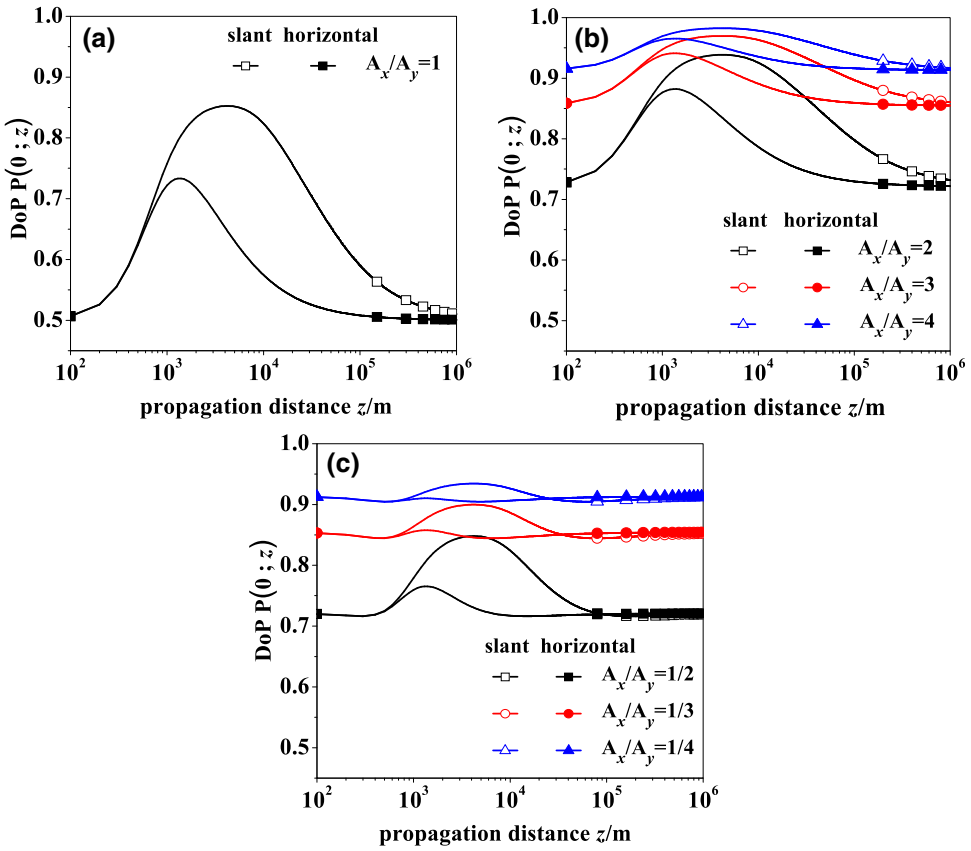

Fig. 6 Axis point DoP P(0; z) with the change in propagation distance z for different amplitude ratios A_x/A_y, (**a**) $A_x/A_y = 1$; (**b**) $A_x/A_y > 1$; (**c**) $A_x/A_y < 1$

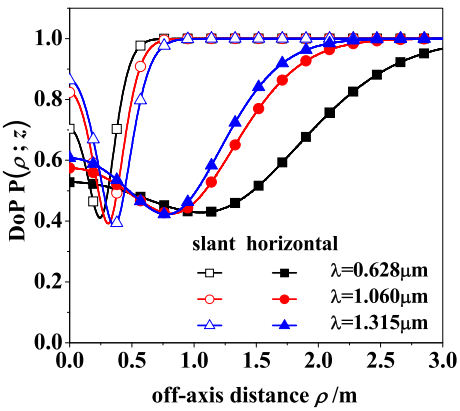

Fig. 7 DoP distribution P(ρ; z) for different wavelengths λ

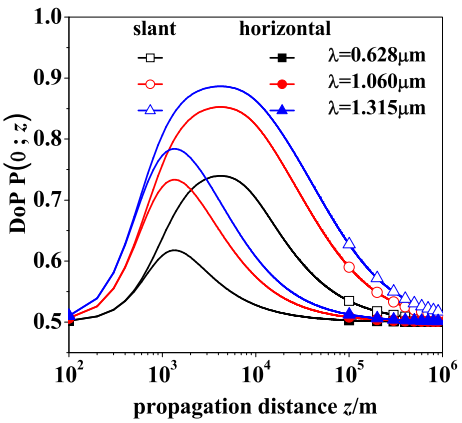

Fig. 8 Axis point DoP P(0; z) with the change in propagation distance z for different wavelengths λ

and Fig. 10 shows the variation in the axis point DoP of the receiver beam with propagation.

In Fig. 9, the DoP distribution of the GSM beam propagating along a slant path is more concentrated than that along a horizontal path. And, the smaller the refractive-index structure constant, the more concentrated the DoP distribution of the receiver beam. It can be seen from Fig. 10 that under the condition of the same C_0, the propagation distance corresponding to the maximum axis point DoP of the GSM propagating along the slant path is longer than that along the horizontal path. Compared to the horizontal path, the detector can receive information at farther distances when the GSM beam propagates along a slant path. In addition, the smaller the refractive-index structure constant, the larger the range of change of the axis point DoP.

In a coherent optical communication system, the inconsistency of the polarization states of the signal light and the local oscillator directly affects the reception sensitivity of the entire system, and the advantages of the coherent optical communication system are weakened.

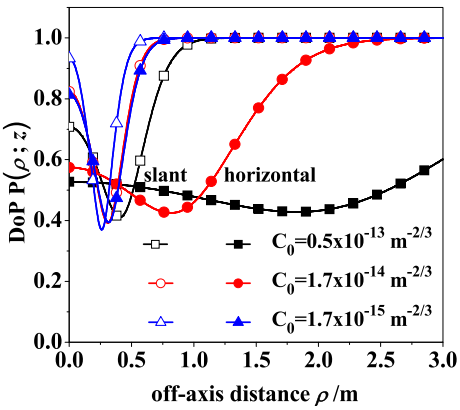

Fig. 9 DoP distribution P(ρ; z) for different refractive-index structure constants C_0

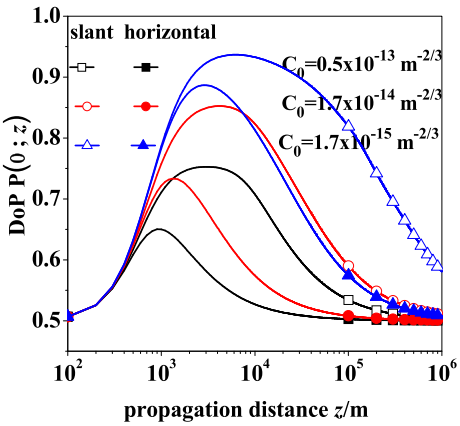

Fig. 10 Axis point DoP P(0; z) with the change in propagation distance z for different refractive-index structure constants C_0

With reference to Figs. 4, 6, 8, and 10, it can be seen that the axis point DoP of the beam propagating over a long distance tends to be constant in the atmospheric turbulence, that is, in a coherent optical system, when the communication distance reaches a certain value, the polarization characteristics of the beam are not affected by the atmospheric turbulence, and the polarization states of the signal light and the local oscillator light can be easily controlled to be consistent.

4. Conclusion

In this study, we analyzed the influence of the light source parameters and atmospheric turbulence on the polarization properties of a partially coherent GSM beam when propagating along a slant path and horizontal path. When $\sigma_x = \sigma_y$, there is a waist radius within 2 cm $< \sigma_x <$ 4 cm that can provide the most concentrated DoP distribution, and the axis point DoP will eventually approach the initial value, implying that it exhibits self-recovery characteristics as the propagation distance increases. Under the conditions of the same light source parameter, the DoP distribution of the GSM beam propagating along the slant path is more concentrated than that along the horizontal path. When the GSM beam propagates along the slant path, the propagation distance corresponding to the maximum axis point DoP is larger; therefore, the detector can receive information at farther distances. Our study can be used as a reference for the selection of light sources and passing information when the GSM beam propagates in atmospheric turbulence. At the same time, it provides an important reference value for the polarization control of atmospheric optical communication systems. Considering the conclusions obtained in this paper regarding the change of the polarization state of a light beam with the propagation distance, future research on coherent optical communication systems should be directed toward understanding how to control the polarization state of local light.

Acknowledgements Project supported by the National Natural Science Foundation of China (NSFC) (61377080, 61771385); Key Industrial Innovation Chain Project of Shaanxi Province (2017ZDCXL-GY-06-01); Xi'an Science and Technology Planning Project (2017080CG/RC043(XALG015)); Natural Science Basic Research Program (2018JQ6032).

References

[1] J L A Perez *IEEE Trans. Geosci. Remote* **49** 426 (2011)
[2] C J Yu and C M Hsieh *IEEE Photonic Technol.* **28** 1229 (2016)
[3] X Tang, Z Ghassemlooy, S Rajbhandari, W O Popoola and C G Lee *J. Lightwave Technol.* **30** 2689 (2012)
[4] G P Agrawal and E Wolf *J. Opt. Soc. Am. A* **17** 2019 (2000)
[5] M Salem, O Korotkova, A Dogariu and E Wolf *Waves Random Media* **14** 513 (2004)
[6] H T Eyyuboğlu, Y Baykal and Y Cai *Appl. Phys. B* **89** 91 (2007)
[7] R Zhang, X Z Wang and X Cheng *Opt. Express* **20** 1421 (2012)
[8] R Zhang, X Z Wang, X Cheng and Z C Qiu *J. Opt. Soc. Am. A* **27** 2496 (2010)
[9] L C Zhang, X Yin and Y Zhu *Optik* **125** 3272 (2014)
[10] M Gao, L Gong and P L Wu *Optik* **125** 4860 (2014)
[11] M Gao, Y Li, H Lv and L Gong *Infrared Phys. Technol.* **67** 98 (2014)
[12] J Ou, Y S Jiang and Y T He *Opt. Laser Technol.* **67** 1 (2015)
[13] E Wolf *Phys. Lett. A* **312** 263 (2003)
[14] O Korotkova and E Wolf *Opt. Commun.* **246** 35 (2005)
[15] H Roychowdghury, S A Ponomarenko and E WOLF *J. Mod. Optic* **52** 1611 (2005)
[16] Y Cui, C Wei, Y T Zhang, F Wang and Y J Cai *Opt. Commun.* **354** 353 (2015)
[17] X H Zhao, Y Yao, Y X Sun and C Liu *Opt. Express* **17** 17888 (2009)
[18] M Verma, P Senthilkumaran, J Joseph and H C Kandpal *Opt. Express* **21** 15432 (2013)
[19] X Du and D Zhao *Opt. Express* **17** 4257 (2009)
[20] Y Zhu and D Zhao *Appl. Phys.* B **96** 155 (2009)
[21] M Luo and D Zhao *Opt. Commun.* **336** 98 (2015)
[22] S Zhu, Y Cai and O Korotkova *Opt. Express* **18** 12587 (2010)

[23] Y Zhao, M Xia, Q Wang, Y Li, Z Hu, H Sun and Y Zhang *Opt. Appl.* **46** 335 (2016)
[24] Y Zhao, Y Zhang, Z Hu, Y Li and D Wang *Opt. Commun.* **371** 178 (2016)
[25] X L Ji and X W Chen *Opt. Laser Technol.* **41** 165 (2009)
[26] T Voipio, T Setala and T Friberg *J. Opt. Soc. Am. A* **30** 71 (2013)
[27] Y P Huang, F H Wang, Z H Gao and B Zhang *Opt. Express* **23** 1088 (2015)
[28] H Y Wang, H L Wang, Y X Xu and X M Qian *Opt. Laser Technol.* **56** 1 (2015)
[29] O Korotkova *Opt. Lett.* **40** 3077 (2015)
[30] O Korotkova and E Wolf *Opt. Lett.* **30** 198 (2005)
[31] X H Zhao, Y Yao, Y X Sun and C Liu *Opt. Express* **17** 17888 (2009)
[32] S C H Wang and M A Plonus *J. Opt. Soc. Am.* **69** 1297 (1979)
[33] L C Andrews and R L Phillips *Laser beam propagation through random media* (Bellingham, 2005)
[34] A Dogariu, E Wolf and T. Shirai *J. Opt. So. Am. A* **20** 1094 (2003)
[35] H Roychowdhury and O Korotkova *Opt. Commun.* **249** 379 (2005)